

Effects of Eu doping on SmB_6 single crystals

Sunmog Yeo,^{1,*} Kimyung Song,² Namjung Hur,^{2,†} Z. Fisk,³ and Pedro Schlottmann⁴

¹*Korea Atomic Energy Research Institute, 150 Dukjin-Dong, Yuseong-Gu, Daejeon, Republic of Korea*

²*Department of Physics, Inha University, Incheon, Republic of Korea*

³*Department of Physics & Astronomy, University of California, Irvine, California 92697, USA*

⁴*Department of Physics, Florida State University, Tallahassee, Florida 32306, USA*

(Received 19 April 2011; revised manuscript received 21 December 2011; published 27 March 2012)

The various phases in $\text{Sm}_{1-x}\text{Eu}_x\text{B}_6$ are investigated based on magnetic susceptibility, resistivity, and Hall effect measurements. The end compounds are a Kondo insulator (SmB_6) and a polaronic ferromagnet (EuB_6). For $x \approx 0.2$, the ground state undergoes a transition from a Kondo insulator to an antiferromagnetic (AF) insulator phase. Further doping induces a transition to an AF metal at $x \approx 0.4$. The spin gap is reduced rapidly with the Eu substitution, while there is a charge gap up to $x \approx 0.4$. The Hall effect indicates a dramatic decrease in the carrier density at low temperatures (T) for the Kondo insulator regime, whereas, the carrier density is almost independent of T in the AF metallic phase.

DOI: [10.1103/PhysRevB.85.115125](https://doi.org/10.1103/PhysRevB.85.115125)

PACS number(s): 75.20.Hr, 71.30.+h, 75.50.Pp

I. INTRODUCTION

The intriguing physical properties of the Kondo insulator SmB_6 and the magnetic-polaron-induced ferromagnetic (FM) phase of EuB_6 have been the topics of numerous papers. The compound $\text{Sm}_{1-x}\text{Eu}_x\text{B}_6$ forms for all values of x and is expected to have a rich phase diagram due to the sensitivity of SmB_6 to pressure^{1,2} and the interplay of FM and antiferromagnetic (AF) correlations. In this paper, we show that, with increasing x , the ground state of $\text{Sm}_{1-x}\text{Eu}_x\text{B}_6$ undergoes a sequence of phase transitions from Kondo insulator to AF insulator to AF metal and finally to the polaron-driven FM state.

SmB_6 is a Kondo insulator with a small gap originating from the hybridization between a narrow f band and broad conduction bands. At ambient pressure, SmB_6 is a homogeneously mixed valence material of valence ~ 2.7 with a ratio of the $4f^6$ to $4f^55d$ configurations of about 3:7.³⁻⁵ The indirect gap of SmB_6 , determined from the resistivity, is approximately 54 K.² There is evidence for intrinsic in-gap bound states from the T dependence of the optical transmission and reflectivity through films,^{6,7} Raman scattering,⁸ neutron-scattering experiments,^{9,10} low- T specific heat,¹¹ and NMR.¹² The in-gap magnetic states have been attributed to magnetic excitations due to AF correlations^{13,14} and could be a signal that SmB_6 is close to an AF instability.¹⁵

On the other hand, EuB_6 is a semimetal at high T undergoing a two-step transition at $T_{c1} \approx 15.3$ K and $T_{c2} \approx 12.6$ K.¹⁶⁻¹⁸ The magnetic transition at T_{c1} is accompanied by a dramatic reduction in the resistivity and is attributed to the formation of a percolative network of magnetic polarons with the concomitant transition from semimetal to metal. The magnetic polarons, i.e., the spins of the carriers polarize the spins of the surrounding Eu^{2+} ions,^{19,20} form in the paramagnetic phase, and grow in size as T is lowered and the field H is increased, giving rise to electronic and magnetic phase separations above T_{c2} .¹⁶⁻¹⁸ A homogeneous FM phase is only established below T_{c2} .

The Sm valence is sensitive to pressure and doping. As a function of pressure, SmB_6 undergoes a first-order phase transition to a magnetically ordered metallic state with features

of the $4f^55d$ configuration at a critical pressure $p_c \approx 6$ GPa.^{1,2} A La^{3+} substitution for Sm causes a decrease in the Sm valence, whereas, a Yb^{2+} substitution increases the Sm valence.²¹ Although Kondo insulators are close to an AF phase transition, these La and Yb substitutions do not give rise to an AF phase nor does a small amount of magnetic doping, such as Eu and Gd.²² However, 5% Sm doping in EuB_6 has been reported to suppress the FM metallic phase and to cause an AF metallic phase.²³ Thus, in view of the competition of FM and AF correlations and the nonmagnetic insulator and FM metallic ground states of the end-point compounds SmB_6 and EuB_6 , the $\text{Sm}_{1-x}\text{Eu}_x\text{B}_6$ system is expected to probe, as a function of x , various magnetic phases and an insulator-to-metal transition.

II. EXPERIMENTAL

Single crystals of $\text{Sm}_{1-x}\text{Eu}_x\text{B}_6$ were grown by an aluminum flux method described in Ref. 24. Powder x-ray diffraction patterns obtained with a Rigaku x-ray diffractometer show that all $\text{Sm}_{1-x}\text{Eu}_x\text{B}_6$ crystals have a single phase cubic structure with space group $Pm\bar{3}m$. The magnetic properties were measured along the cubic axis in a commercial superconducting quantum-interference device magnetometer. The resistivity was obtained with a standard four-probe technique, and the Hall coefficient was measured by a Quantum Design physical properties measurement system with the current along the $\langle 100 \rangle$ direction. In order to remove the longitudinal magnetoresistance in Hall measurements, opposite field measurements also were performed at the same T .

III. RESULTS

Figure 1 shows the phase diagram of $\text{Sm}_{1-x}\text{Eu}_x\text{B}_6$ obtained from magnetic, transport, and Hall measurements. For $x < 0.4$, the solid diamonds represent the transport (or charge) gaps from the T dependence of the electrical resistivity $\rho(T)$ as discussed below. The AF transition temperature, T_N is determined by the maximum T of $d\chi/dT$, which is symbolized by the solid circles in Fig. 1. The open triangles

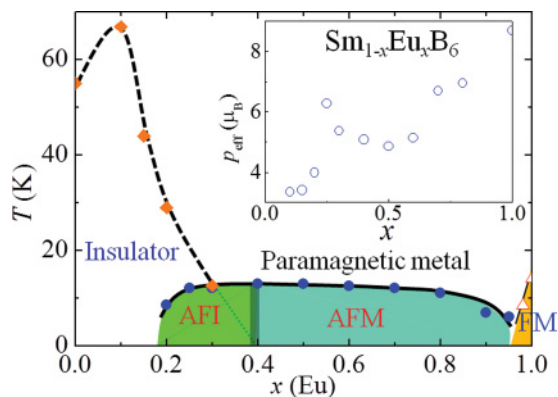


FIG. 1. (Color online) Phase diagram of $\text{Sm}_{1-x}\text{Eu}_x\text{B}_6$. Solid diamonds, solid circles, and open triangles correspond to the transport gap, the Néel, and the Curie temperatures, respectively. The vertical dashed line is a guide to the eye for the phase boundary between the AF insulator and the AF metal. The insulating phase for small x originates from the Kondo insulator SmB_6 . The inset shows the effective moment for $\text{Sm}_{1-x}\text{Eu}_x\text{B}_6$.

show the Curie temperature of the FM transitions obtained from the minimum of $d\chi/dT$. The transition from the Kondo insulator to the AF insulator occurs at $x \approx 0.2$.

Figure 2(a) and the inset of Fig. 2(a) show $\chi(T)$ for $x \leq 0.25$. The Curie tail in SmB_6 at low T is characteristic of Kondo insulators and is attributed to the intrinsic in-gap states.

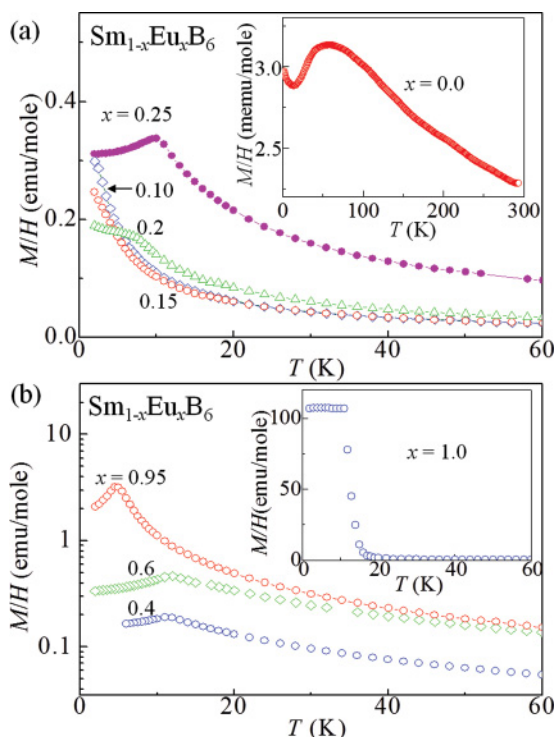


FIG. 2. (Color online) (a) T dependence of M/H for $x = 0.1, 0.15, 0.2$, and 0.25 , where $H = 100$ Oe. M/H for SmB_6 is shown in the inset. (b) T dependence of M/H for $x = 0.4, 0.6$, and 0.95 , where $H = 100$ Oe. The inset displays M/H for EuB_6 .

At intermediate T , $\chi(T)$ displays a hump at ~ 55 – 60 K [see the inset of Fig. 2(a)], which also is characteristic of Kondo insulators and is determined by the spin gap, i.e., the indirect hybridization gap. At low T , the susceptibility of SmB_6 is the superposition of the Curie law of the in-gap states, a T -independent Van Vleck contribution and an Arrhenius law for the activation across the hybridization gap. It is difficult to separate these three contributions, and this hinders the data analysis to extract the spin gap Δ_s . In the T range between 40 and 150 K, on the other hand, $\chi(T)$ is of the form

$$\chi(T) = (C/T) \exp(-\Delta_s/k_B T) + \chi_0. \quad (1)$$

A fit of the data to this expression is shown in Fig. 3(a) by the solid curve and yields $\Delta_s \sim 58$ K, which is consistent with the spin gap obtained in Refs. 12 and 25 where gaps in the range of 55–65 K were obtained. The activation gap explains the hump at ~ 55 K in the data. The quality of the fit is limited in the range of 40–50 K by the intrinsic in-gap states and, at higher temperatures, by the closing of the gap (Kondo-like many-body effects are weakened with T).

$\chi(T)$ for $x = 0.1$ just displays paramagnetic behavior up to 300 K without the expected hump. The effective Curie constant $T\chi$ as a function of T is displayed in Fig. 3(b). It is seen that $T\chi$ is reduced by more than a factor of 2 when the temperature is lowered from 60 to 2 K. A possible explanation of this temperature dependence is a reminiscent Kondo spin gap, which is very difficult to determine quantitatively because of the intrinsic in-gap bound states, and the large magnetic

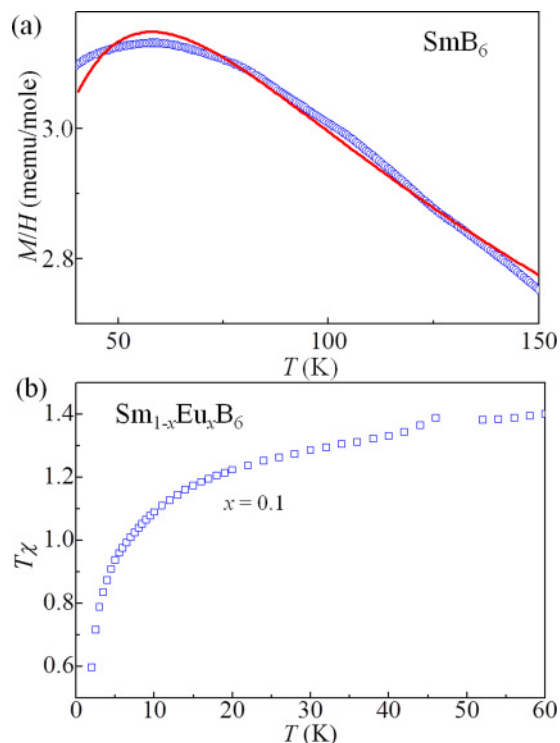


FIG. 3. (Color online) (a) The magnetic susceptibility data between 40 and 150 K for $x = 0.0$. The solid curve is a fit curve to $\chi(T) = (C/T) \exp(-\Delta_s/k_B T) + \chi_0$. (b) Effective Curie constant $T\chi(T)$ for $x = 0.1$ as a function of temperature.

moments of the Eu^{2+} ions tend to close the spin gap.²⁶ In any case, if this feature is due to a spin gap, this gap would be rather small, possibly on the order of a few degrees, suggesting that Δ_s of SmB_6 is fragile against Eu substitution.

Interestingly, further doping with Eu introduces a kink at ~ 8 K for $x = 0.2$ and a clear downturn at ~ 13 K for $x = 0.25$ indicating that sufficient Eu doping causes a transition to an AF state. Indeed, as shown in Fig. 2(b), further Eu doping displays a clear AF transition for $0.25 < x \leq 0.95$. Note that no significant deviation was observed between zero-field cooling and field cooling measurements (not shown here), which is an indication that the transition is of second order and not of the spin-glass type. In contrast to the AF transition, $x = 1.0$ displays a ferromagnetic transition as shown in the inset of Fig. 2(b). The AF-to-ferromagnetic transition is discussed in Ref. 23. It is interesting to point out that no indication of an AF state was found for the $x = 0.15$ and $x = 0.1$ samples down to 2 K, suggesting that the onset of AF is quite abrupt around or above $x = 0.15$. The disappearance of the AF order is due to the dilution of the Eu^{2+} moments and possibly as well due to the competition of AF with the reminiscent Kondo insulator gap.

The effective moment for $x \leq 1$ is obtained by fitting the high- T region ($T > 100$ K) of the susceptibility with a Curie-Weiss law and is displayed in the inset of Fig. 1. The effective moment jumps in the vicinity of the AF transition, which could be associated with a change in valence of the Sm ions. As expected, the effective moment for $0.5 \leq x \leq 1$ increases monotonically with the Eu concentration.

The T dependence of the resistivity for $x \leq 0.3$ is shown in Fig. 4(a). For $x = 0.2$, although $\chi(T)$ has a kink at ~ 8 K, $\rho(T)$ behaves like a normal insulator at all T . For $x = 0.3$, the T dependence of the resistivity is insulatorlike but tends to saturate below the Néel temperature. This phase then corresponds to a (mostly gapless) Kondo insulator. Further Eu doping gives rise to an insulator-metal transition, shown in the inset of Fig. 4(a). The resistivity for $0.4 \leq x \leq 0.8$ displays metal-like T dependence and an accompanying drop near the AF phase transition. If we extrapolate the transport gap to its zero value concentration, we obtain $x_{MI} \sim 0.4$ for the insulator-metal transition.

The transport gap Δ_t is determined from the thermal activation law,

$$\rho(T) = \rho_0 \exp(\Delta_t/2k_B T), \quad (2)$$

and is obtained by fitting $\ln \rho(T)$ vs $1/T$ for $20 \text{ K} < T < 50 \text{ K}$ as shown in Fig. 4. For $x = 0$, we have $\Delta_t \sim 55$ K in reasonable agreement with previous papers.²⁷ Note that, for a pure Kondo insulator, the spin and charge gaps are expected to be equal, showing that our analysis is consistent. As a function of x , Δ_t displays a peak at $x = 0.1$, and then, the transport gap decreases with increasing x and vanishes around $x = 0.4$. This is consistent with the hard photoemission spectroscopy data from Ref. 28, which show that the gap for $x = 0.15$ is only a little smaller than for $x = 0$, and for $x = 0.5$, there is no trace of a Kondo peak.

Note that, for SmB_6 , like for other Kondo insulators, the spin and transport gaps have almost the same value since their common origin is the hybridization of the bands. However,

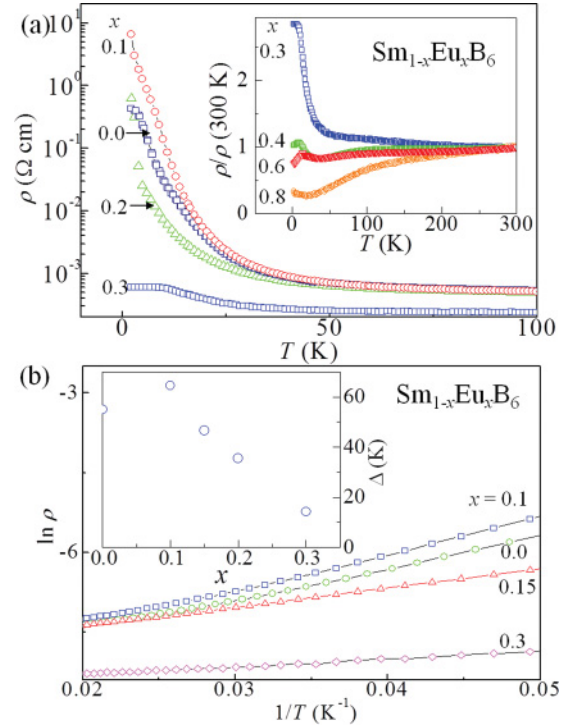


FIG. 4. (Color online) (a) T dependence of the resistivity for $x = 0.0, 0.1, 0.2$, and 0.3 . The inset displays $\rho/\rho(300 \text{ K})$ for $x = 0.3, 0.4, 0.6$, and 0.8 . (b) Thermal activation of $\rho(T)$ for $x \leq 0.3$. The transport gaps are shown in the inset.

the spin and transport gaps for the doped materials are often different due to the distinct ways disorder affects the quantities. The inset of Fig. 4(b) summarizes the results for the transport gap (open circles) of $\text{Sm}_{1-x}\text{Eu}_x\text{B}_6$. The initial increase in Δ_t with x probably arises from the mobility edges due to disorder scattering in the conduction and valence bands, i.e., Δ_t represents the mobility gap rather than the band gap. For $0.2 < x < 0.4$, there still is a transport gap, although the spin gap already is closed. In this concentration range, the Eu substitution gives rise to an AF insulating phase. Attempted fits of the resistivity to the variable range hopping expression were not successful.

For a Kondo insulator, such as SmB_6 , the number of carriers should increase with T due to the thermal activation across the gap. This can be verified by extracting the Hall coefficient (R_H) at different T 's as shown in the inset Fig. 5(a). R_H of SmB_6 , plotted as a function of $1/T$, shows two intervals of the activation behavior, $5 \text{ K} < T < 15 \text{ K}$ and $T > 15 \text{ K}$, which is consistent with previous Hall resistance measurements.^{2,4,27} The slope of ρ_H for SmB_6 increases rapidly with decreasing T , suggestive of a drastic reduction in the carriers [see the inset of Fig. 5(a)]. Since the valence and conduction bands contribute with carriers, a two-band model is necessary to qualitatively interpret these results. Within the relaxation time approximation and assuming that there are as many electrons as holes, the negative slopes imply that $\tau_e/m_e > \tau_h/m_h$ so that the electrons in the conduction band are the dominant carriers at low T . Neglecting the contribution of the holes, the T dependence of the electron density (n_e) can be obtained using the simple single-band model and is shown in Fig. 5(b).

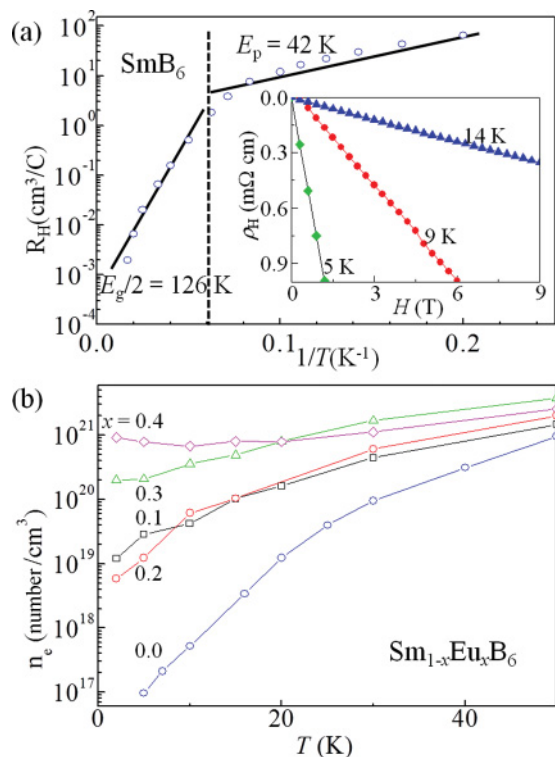


FIG. 5. (Color online) (a) The Hall coefficient for SmB_6 vs $1/T$. E_p and E_g indicate the intragap bound-state binding energy and charge gap, respectively.²⁷ The inset displays the Hall resistivity for selected T . (b) Carrier density as a function of T for $x \leq 0.4$.

For SmB_6 , the carrier density at 5 K is $\sim 1 \times 10^{17}/\text{cm}^3$, which is consistent with previous measurements,² i.e., about 1×10^4 times smaller than that at 50 K. For $x = 0.1$ and 0.2 , on the other hand, the carrier density at 5 K is about 100 times smaller than that at 50 K. This is consistent with the Kondo insulator picture when the gap is filled with impurity states.²⁶ However, further doping shows that n_e is independent of T , indicating that the system is no longer a Kondo insulator for $x > 0.2$.

IV. DISCUSSION

At first glance, it is surprising that, for SmB_6 , the gap obtained from R_H is so much larger than the transport gap Δ_T . This is, however, consistent with the results reported in Ref. 27 for the same compound. Assuming a compensated semiconductor, i.e., as many electrons as holes, the ratio $R_H/\rho = \mu_h - \mu_e$, i.e., the difference in the mobilities of holes and electrons has to have an exponential T dependence rather than the usually expected power law of T . This is indicative of a mobility edge playing a role even for $x = 0$.

The bulk-sensitive hard x-ray photoelectron spectroscopy for $\text{Sm}_{1-x}\text{Eu}_x\text{B}_6$ suggests that an increase in the Eu concentration decreases the strength of the hybridization and, hence, increases the Sm valence.²⁹ When the conduction band weakly hybridizes with highly correlated electronic states, two different but related interactions may occur:³⁰ If the system is

metallic, the interaction is of the Ruderman-Kittel-Kasuya-Yosida type and is oscillatory with distance, whereas, in an insulator, the interaction is related to the AF superexchange and falls off exponentially with distance. The relation between these mechanisms can be understood by considering the k_F of an insulator as an imaginary quantity so that the $\cos(2k_F R)$ oscillations become an exponentially falloff with R . In SmB_6 , due to the intermediate valence, the hybridization between localized f electrons and conduction electrons is strong, and hence, the ground state is nonmagnetic. However, Eu doping weakens the hybridization and, thus, the magnetically active ions, Sm and Eu ions, can interact with each other. On the insulator side, these interactions will be AF and will give rise to an AF insulator at $x \approx 0.2$ in $\text{Sm}_{1-x}\text{Eu}_x\text{B}_6$. With increasing x , the charge gap is closed, yielding a metallic state. Due to strong disorder, the interaction is still short ranged and predominantly AF. Only when the system is close to EuB_6 ($x \approx 1.0$), FM polarons can form and eventually can percolate to a FM ground state.^{16–18}

It is interesting to compare $\text{Sm}_{1-x}\text{Eu}_x\text{B}_6$ to $\text{Ca}_{1-x}\text{Eu}_x\text{B}_6$. Both SmB_6 and CaB_6 are nonmagnetic insulators, but CaB_6 is a large-gap insulator without the complications of a Kondo insulator. For small x , due to the broken translational invariance, the Eu ions in $\text{Ca}_{1-x}\text{Eu}_x\text{B}_6$ give rise to bound states in the gap.²⁶ With increasing x , these bound states overlap and eventually percolate giving rise to metallic behavior at low T for $x > 15\%$.^{31,32} Magnetic polarons start to form, and at $x \approx 0.3$, $\text{Ca}_{1-x}\text{Eu}_x\text{B}_6$ becomes a FM metal.^{31,32} Phase separation between Ca-rich and Eu-rich regions has been found around $x \approx 0.3$ by electron microscopy (Ref. 31) and via electron spin resonance for smaller x .³² In $\text{Sm}_{1-x}\text{Eu}_x\text{B}_6$, the small gap and the hybridization favor an AF interaction between magnetic ions, leading to an AF insulating phase at $x \approx 0.2$. Each Eu ion introduces a bound state into the gap of the Kondo insulator. The metal-insulator transition in $\text{Sm}_{1-x}\text{Eu}_x\text{B}_6$ could then be interpreted as a percolation of bound states similar to $\text{Ca}_{1-x}\text{Eu}_x\text{B}_6$.

To summarize, we investigated Eu-doping effects in SmB_6 based on the magnetic susceptibility, resistivity, and Hall effect measurements. Since Eu doping reduces the strength of the hybridization between a narrow f band and broad conduction bands, an AF superexchange interaction appears between magnetically active ions, causing a transition from a Kondo insulator to an AF insulator at $x \approx 0.2$. With further Eu doping, the percolation into a metallic state is reached at $x \approx 0.4$. Finally, for Eu-rich samples, a transition from the AF metal to a FM metal is observed at $x \approx 0.95$. For $x > 0.95$, magnetic polarons can form and can percolate to yield a FM phase.

ACKNOWLEDGMENTS

S.Y. is supported by the Proton Engineering Frontier Project and Radiation detector development project sponsored by the Ministry of Education, Science and Technology (MEST) and a grant from the Fundamental R&D program from Core Technology of Materials funded by the Ministry of Knowledge Economy (MKE). P.S. is supported by the US Department of Energy through Grant No. DE-FG02-98ER45707.

*sunmog@gmail.com

†nhur@inha.ac.kr

- ¹A. Barla, J. Derr, J. P. Sanchez, B. Salce, G. Lapertot, B. P. Doyle, R. Ruffer, R. Lengsdorf, M. M. Abd-Elmeguid, and J. Flouquet, *Phys. Rev. Lett.* **94**, 166401 (2005).
- ²J. C. Cooley, M. C. Aronson, Z. Fisk, and P. C. Canfield, *Phys. Rev. Lett.* **74**, 1629 (1995).
- ³J.-N. Chazalviel, M. Campagna, G. K. Wertheim, and P. H. Schmidt, *Phys. Rev. B* **14**, 4586 (1976).
- ⁴J. W. Allen, B. Batlogg, and P. Wachter, *Phys. Rev. B* **20**, 4807 (1979).
- ⁵E. Beaurepaire, J. P. Kappler, and G. Krill, *Phys. Rev. B* **41**, 6768 (1990).
- ⁶T. Nanba, H. Ohta, M. Motokawa, S. Kimura, S. Kunji, and T. Kasuya, *Physica B* **186–188**, 440 (1993).
- ⁷B. Gorshunov, N. Sluchanko, A. Volkov, M. Dressel, G. Knebel, A. Loidl, and S. Kunii, *Phys. Rev. B* **59**, 1808 (1999).
- ⁸P. Nyhus, S. L. Cooper, Z. Fisk, and J. Sarrao, *Phys. Rev. B* **55**, 12488 (1997).
- ⁹P. A. Aleckseev, J.-M. Mignot, J. Rossat-Mignod, V. N. Lazukov, I. P. Sadikov, I. P. Sadikov, E. S. Konovalova, and Y. B. Paderno, *J. Phys.: Condens. Matter* **7**, 289 (1995).
- ¹⁰A. Bouvet, T. Kasuya, M. Bonnet, L. P. Regnault, J. Rossat-Mignod, F. Iga, B. Fåk, and A. Severing, *J. Phys.: Condens. Matter* **10**, 5667 (1998).
- ¹¹S. von Molnár, T. Theis, A. Benoit, A. Briggs, J. Flouquet, and J. Ravex, in *Valence Instabilities*, edited by P. Wachter and H. Boppert (North-Holland, Amsterdam, 1982), p. 389.
- ¹²T. Caldwell, A. P. Reyes, W. G. Moulton, P. L. Kuhns, M. J. R. Hoch, P. Schlottmann, and Z. Fisk, *Phys. Rev. B* **75**, 075106 (2007).
- ¹³P. S. Riseborough, *Phys. Rev. B* **68**, 235213 (2003).
- ¹⁴P. S. Riseborough, *Annalen der Physik* **9**, 813 (2000).
- ¹⁵V. Dorin and P. Schlottmann, *Phys. Rev. B* **46**, 10800 (1992).
- ¹⁶S. Süllo, I. Prasad, M. C. Aronson, J. L. Sarrao, Z. Fisk, D. Hristova, A. H. Lacerda, M. F. Hundley, A. Vigliante, and D. Gibbs, *Phys. Rev. B* **57**, 5860 (1998).
- ¹⁷S. Süllo, I. Prasad, M. C. Aronson, S. Bogdanovich, J. L. Sarrao, and Z. Fisk, *Phys. Rev. B* **62**, 11626 (2000).
- ¹⁸L. Degiorgi, E. Felder, H. R. Ott, J. L. Sarrao, and Z. Fisk, *Phys. Rev. Lett.* **79**, 5134 (1997).
- ¹⁹P. Nyhus, S. Yoon, M. Kauffman, S. L. Cooper, Z. Fisk, and J. L. Sarrao, *Phys. Rev. B* **56**, 2717 (1997).
- ²⁰R. Urbano, P. G. Pagliuso, C. Rettori, S. B. Oseroff, J. L. Sarrao, P. Schlottmann, and Z. Fisk, *Phys. Rev. B* **70**, 140401(R) (2004).
- ²¹M. Kasaya, J. M. Tarascon, and J. Etourneau, *Solid State Commun.* **33**, 1005 (1980).
- ²²T. H. Geballe, A. Menth, E. Buehler, and G. W. Hull, *J. Appl. Phys.* **41**, 904 (1970); T. Uemura, Y. Chiba, S. Kunii, M. Kasaya, T. Kasuya, and M. Date, *J. Phys. Soc. Jpn.* **55**, 43 (1986).
- ²³S. Yeo, J. E. Bunder, H.-H. Lin, M.-H. Jung, and S.-I. Lee, *Appl. Phys. Lett.* **94**, 042509 (2009).
- ²⁴Z. Fisk, D. C. Johnston, B. Cornut, S. von Molnár, S. Oseroff, and R. Calvo, *J. Appl. Phys.* **50**, 1911 (1979).
- ²⁵V. V. Glushkov, A. V. Kusnetsov, O. A. Churkin, S. V. Demishev, Y. B. Paderno, N. Y. Shitsevalova, and N. E. Sluchanko, *Physica B* **378–380**, 614 (2006).
- ²⁶P. Schlottmann, *Phys. Rev. B* **46**, 998 (1992).
- ²⁷N. E. Sluchanko, V. V. Glushkov, S. V. Demishev, A. A. Pronin, A. A. Volkov, M. V. Kondrin, A. K. Savchenko, and S. Kunii, *Phys. Rev. B* **64**, 153103 (2001).
- ²⁸J. Yamaguchi, A. Sekiyama, M. Y. Kimura, H. Sugiyama, Y. Tomida, G. Funabashi, S. Komori, T. Balashov, W. Wulfhekel, T. Ito, S. Kimura, A. Higashiya, K. Tamasaku, M. Yabashi, T. Ishikawa, S. Yeo, S.-I. Lee, F. Iga, T. Takabatake, and S. Suga, e-print arXiv:1002.2530.
- ²⁹J. Yamaguchi, A. Sekiyama, S. Imada, A. Higashiya, K. Tamasaku, M. Yabashi, T. Ishikawa, T. Ito, S. Kimura, F. Iga, T. Takabatake, S. Yeo, S.-I. Lee, H.-D. Kim, and S. Suga, *J. Phys.: Conf. Ser.* **200**, 12230 (2010).
- ³⁰C. G. da Silva and L. M. Falicov, *J. Phys. C* **5**, 63 (1972).
- ³¹G. A. Wigger, C. Beeli, E. Felder, H. R. Ott, A. D. Bianchi, and Z. Fisk, *Phys. Rev. Lett.* **93**, 147203 (2004).
- ³²R. R. Urbano, P. G. Pagliuso, C. Rettori, P. Schlottmann, J. L. Sarrao, A. Bianchi, S. Nakatsuji, Z. Fisk, E. Velazquez, and S. B. Oseroff, *Phys. Rev. B* **71**, 184422 (2005).